



Light guidance film for bifacial photovoltaic modules

Markus Zauner^{a,*}, Wolfgang Muehleisen^a, Dominik Holzmann^a, Marcus Baumgart^a, Gernot Oreski^b, Sonja Feldbacher^b, Markus Feichtner^c, Wolfgang Nemitz^d, Claude Leiner^d, Christian Sommer^d, Frank Reil^d

^a Silicon Austria Labs GmbH, Europastr.12, Villach/St.Magdalen, 9524, Austria

^b Polymer Competence Center Leoben GmbH, Roseggerstrasse 12, 8700, Leoben, Austria

^c KIOTO GmbH, Wernersdorf 111, 8551, Wies, Austria

^d Joanneum Research, Weiz, Austria

ARTICLE INFO

Article history:

Received 21 May 2021

Received in revised form

31 August 2021

Accepted 16 September 2021

Available online 21 September 2021

Keywords:

PV Modules

Light guidance film

Bifacial

Characterization

ABSTRACT

To improve the efficiency of bifacial photovoltaic modules, the idea of light deflection was addressed. A thin film with an intended structure was applied in the space between the cells. Due to the selected structural geometry, unused light is specifically redirected to the solar cell and can be absorbed by it and converted into additional current. The effect of the light-directing film was both simulated and measured. Single PV modules without and with commercial structured films or white back sheet were measured to evaluate the results. The expected gain of up to 11% from the simulation could not be achieved by measurement, by reaching about 3%.

© 2021 Elsevier Ltd. All rights reserved.

1. Introduction

For the manufacturers of photovoltaic (PV) modules, the continuous improvement of efficiency is important to survive in the regional and international market. Light management and guidance within the PV module is one approach for increasing the module efficiency by increasing the number of photons coming to the solar cell. Over the years different approaches have been investigated for monofacial solar cells. For example, the light guiding effect of structured front sheets made of polycarbonate (PC) or polymethyl methacrylate (PMMA), which replace the front glass, has been tested [1–3]. However, none of these approaches have been adopted by the PV industry due to issues in long term stability, thermo-mechanical behaviour and compatibility with the encapsulation material. Other approaches address the optical shadowing of the solar cell grid fingers and busbars, ranging from a local change of the optical properties in the bulk of the photovoltaic module encapsulation material [4,5] to structured ribbons [6,7]. Also backscattering via a diffuse reflecting white back sheet has been exploited [8].

According to the report from “International Technology Roadmap for Photovoltaics” of 2020, the sales market for bifacial modules will grow steadily over the next 30 years [9]. In comparison to conventional modules, the solar cells are embedded between two glass sheets in EVA and not between a glass sheet and a white back sheet. This design allows reflecting light from e.g., concrete, metal, or grass to be absorbed by the back of the cell, generating up to 30% more power. The surface of a standard PV module is usually covered with 85% of cells and is directly hit by the sun’s rays. In the intermediate areas between the cells and in the edge areas, the light exits on the rear side and only the rays reflected by the ground can be used to generate energy. The remaining light is lost. Several research teams have already set themselves the target of making the best possible use of this light. By using a reflective layer, a research team from England has already been able to simulate the positive effect of light guidance.

The layer was inserted and simulated at three different positions (outside back glass, inside back glass and at the height of the solar cell). Depending on the position and layer width, a gain of 1.7–2.2% could be achieved [10]. In 2017, a group from Germany was able to redirect the sun’s rays by using a structured back sheet and thus achieve an additional gain of 2.5% compared to a white back sheet [11]. In 2018, the research partner Joanneum Research developed

* Corresponding autho.

E-mail address: markus.zauner@silicon-austria.com (M. Zauner).

a reflective layer of silver that was laminated underneath the solar cell, which redirects the light rays to the rear side or, by total reflection, to the top side of the solar cell. Using this, a gain of 2–6% could be achieved by means of laboratory tests [4,12].

Based on the basic principle of light deflection and the geometries developed in the previous project [12] a new approach for light guidance for bifacial PV modules is presented within this paper. The light guidance is achieved by using a structured film, which is produced by extrusion on a patterned extrusion chill roll. The resulting structured film is later attached to the outside of the rear glass of a bifacial PV module using a transparent adhesive. In comparison to the other approaches, this film can also be applied to already existing modules and does not lead to shading due to the intended material. The optical behavior of the adhered structured film and the interaction with the solar cells was simulated.

A comprehensive market and literature review was done to identify and select possible candidate materials for the film and glue. The extruded and embossed film was tested for optical properties, thermal expansion behavior, structural fidelity and roughness and then bonded to the back of a test module and tested under laboratory and real conditions. Tests performed under laboratory and real conditions served as comparative measurements to the simulations.

2. Methodology

2.1. Light guiding structure

The light guiding structures are located on a film, which is optically bonded to the less sunlight-exposed side (i.e. backside) of the bifacial module to reflect light passing through the interstices of the PV elements, towards the backside of the PV elements. The structure is composed of linearly extruded triangles (saw tooth shape) with base angles of 45° and 85° and a height of 150 μm. The direction of reflection depends on the orientation of the structure, making it possible to reflect incident light to both the left and right PV elements by mirroring the structure on the axis of symmetry. The optical functionality of the structures is based on a combination of total internal reflection (TIR) and refraction. Fig. 1 illustrates this combination for the case of perpendicular incident light rays (black dotted arrows).

The light rays hit the 45° edges of the structure and are reflected due to TIR towards the 85° edge where they leave the substrate. Subsequently, the light rays re-enter the substrate at the 45° edge of the adjacent triangle. Depending on their initial point of entry, the rays keep on re-entering the substrate at different triangles, resulting in a broad angular distribution of the reflected light field. By applying the film to the back of a PV module, the rays are directed to the back side or to the top side of the solar cell.

2.2. Material requirements

The material for the structured film must fulfill several requirements with respect to its optical properties, dimension

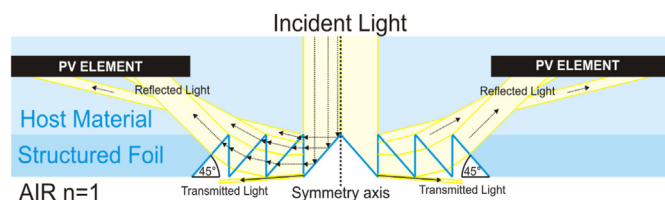


Fig. 1. Schematic illustration of the optical functionality of the light guiding structures for perpendicular incident light.

stability and long-term stability. To match the spectral response of a silicon solar cell, a transmittance higher than 90% is aspired between 300 and 1100 nm wavelength range [13]. To enable effective light guidance the haze of the film should not exceed 5%. Next to the optical properties, dimension stability over the whole temperature range from –20 °C to about 80 °C [14] is crucial for the efficiency of the light guiding effect. The film material should have a low and more or less isotropic coefficient thermal expansion without any significant warpage. Additionally, the material needs to have high resistance towards UV radiation, not showing any yellowing after 50 kWh/m² of UV dosage (between 300 and 400 nm). The adhesive for attaching the structured film to the PV module has to provide a similar property profile with respect to optical properties and dimension stability. Additional aspects are the compatibility between the adhesive and the respective film material and the ease of application.

3. Experimental & methods

3.1. Materials selection

The first step was to select suitable materials for use as light-guidance films used on photovoltaic modules. A comprehensive literature and market review, based on the requirements profile, lead to the selection of four different materials for further investigation:

- Polypropylene (PP) – 510 μm
- Polyamide 12 (PA12) – 600 μm
- Polycarbonate (PC) – 510 μm
- Polymethylene methyl acrylate (PMMA) – 500 μm

Other materials such as polyester (PET) [15,16] or fluoropolymers such as Ethylene tetrafluoroethylene (ETFE) or Polyvinylidene fluoride (PVDF) [17] also meet the technical requirements according to the research, but were excluded for processing and economic reasons. Standard and structured films have been extruded using a laboratory single screw extruder where the material is embossed at the end using two heated rolls (pressure & structure roll). This device was able to produce a maximum film width of 6 cm.

The following commercially available transparent adhesives were tested for bonding the structured films to the back glass in PV modules.

3.2. Material testing

The CTE (Coefficient of thermal expansion) is measured using a Dantec Q400 Digital Image Correlation (DIC) system. Digital Image Correlation (DIC) systems enable contactless and precise measurement of thermally and/or mechanically induced strains of thin as well as anisotropic layers [18,19]. DIC systems are optical strain measurement systems, using a camera setup and specimens with a random speckle pattern. The camera(s) can track this specific speckle pattern and hence the deformations of samples during loading can be measured similarly in two directions. The samples are placed horizontally on a hotplate. The hotplate is placed within a concealed temperature chamber. All DIC samples are painted with a white primer. Afterwards, the pattern was applied using a dedicated black graphite DIC aerosol lacquer. All CTE measurements are done between 20 °C and 150 °C.

The optical properties of the single backsheet films were measured using a Lambda 950 UV/VIS/NIR spectrometer (PerkinElmer). Spectra were recorded from 250 nm to 2500 nm with an

integrating sphere from Labsphere in order to measure hemispheric and diffuse transmittance values.

To determine the suitability of these adhesives for joining of glass plates with polycarbonate (PC) films, pre-test (visual inspection, manual peeling) as well as standardized peel tests were performed. For the preparation of the specimens, 1.5 cm wide and 15 cm long polycarbonate strips were glued to 5 cm wide and 15 cm long glass plates, using the adhesives listed in Table 1. After the application of the adhesive on the glass the selected light guidance films were applied with low manual pressure to generate an adhesive layer thickness of approx. 200 μm. Before that, a cleaning step was carried out: acetone was used for the glass plate and diluted ethanol for the polycarbonate material. Masking tape was used to prevent the adhesive from running over the polycarbonate strip. The adhesives were cured for seven days at room temperature.

These peel tests were performed on an Instron 5500 machine (Instron Deutschland GmbH) with a 100 N or 1 kN load cell. Since the film was very stiff, a peel angle (angle between film and substrate) of 30° was selected. The clamping pressure of the film was 5 bar. The measurements were carried out at the beginning with a crosshead speed of 1 mm/min. The peel force was determined as the mean value of the plateau of the force-displacement diagram over a longer section of the crosshead path.

3.3. Structuring

The aluminum extrusion is structured using picosecond laser ablation. In this technique, pulsed laser light (1064 nm wavelength, average power 100 W, pulse length 10 ps, pulse energy 90 μJ) is focused onto the surface of the rotating roll (180 rpm), see Fig. 2. At the focal spot, material is rapidly heated up and ejected, the total amount of which depends on pulse energy, pulse rate and exposure time. By advancing the beam in axial direction while modulating the deposited energy, a 20 mm wide saw-tooth structure as provided in section 2.1 has been created in the center of the roll. Fig. 3 shows the cross-section (W × H of 1.5 mm × 0.5 mm) of a silicone molding of the resulting structure.

Ultrashort laser pulses usually produce a surface roughness not suitable for optical applications due to the violent nature of material ejection. In addition, roughness increases with the rate of ejected volume, highlighting the trade-off between required production time and surface smoothness. Here and in general, intelligent, individually tailored scanning techniques and choice of laser parameters can improve the surface quality significantly. Rotating the roll in the process decreases the degrees of freedom for such techniques due to the fixed direction and speed along its circumference. Nevertheless, a mean roughness Ra of 1.5 μm was obtained with this technique.

3.4. Simulations

To evaluate the structure in three-dimensional space, an optical simulation was performed using OpticStudio from Zemax. For the simulation, the basic calculation “ray tracing” was used. The sun

Table 1
Selected commercial adhesives.

Name	Characteristics
Adhesive 1	Silicone, one component, high viscosity
Adhesive 2	Polyurethane based, two components
Adhesive 3	Synthetic elastomer based
Adhesive 4	Silicone, two components, RT crosslinking
Adhesive 5	Silicone, two components, RT crosslinking

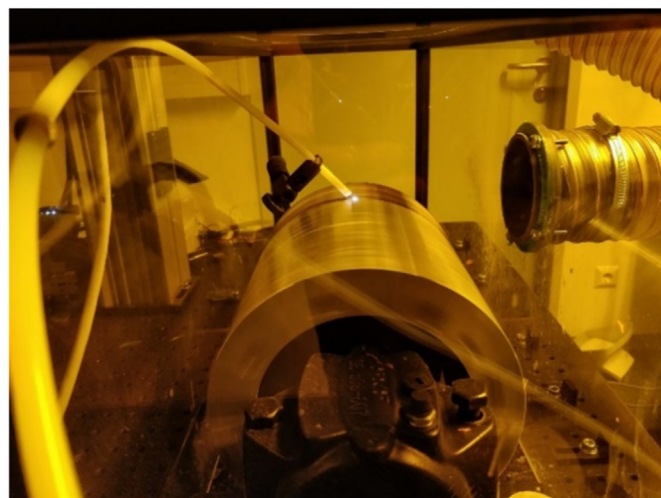


Fig. 2. High intensity pulsed laser light is incident onto the rotating extrusion role, producing a white plasma plume at its surface where material is ejected. The white tube on the left directs a stream of compressed air onto the focal spot to remove debris, which would otherwise block the laser light.

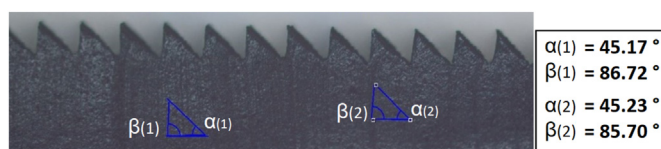


Fig. 3. Cross-section of a silicone molding of part of the finished saw-tooth structure on the role.

was described to the terrestrial solar radiation (air mass AM1.5) [20]. To keep the simulation time within a reasonable range, a step width of 50 nm was chosen for the wavelength meshing between 400 nm and 1050 nm.

The discrete wavelength steps are so wide that no significant contributions/changes from peaks in the AM1.5 spectrum are to be expected. Regarding optical effects of the materials, the following parameters were defined: the glass, EVA, adhesive and the structured film are transparent and non-absorbent, that the light can reach the solar cell without losses. The reflection coefficient from air to glass and vice versa is assumed to be 4%. Scattering on rough surfaces is not considered. For the qualitative evaluation of the light guiding sawtooth structure, the influence of several different structure angles and adhesive thicknesses were simulated. Furthermore, the performance of three differently structured films was measured to show the advantages of the selected structure.

3.5. Test structure

To validate the set-ups and as comparative measurements for the light guiding structure, commercial films were used. The following table shows the films used and their surface structure. A white back sheet is used in monofacial PV modules as a protective layer for the transparent EVA encapsulation film. The other three films are used for light management. These are used in targeted light control for luminaires as well as for packaging, mouse pads or displays. The exact structure of the ECOCAN film cannot be described in detail due to the confidentiality of the project. However, it can be seen from the picture that this is a sawtooth geometry running outwards with decreasing spacing. For the simulations the geometry of the structures was digitized and for

the laboratory and outdoor tests, the films were cut into strips of various widths, and bonded to the edge areas or areas between two cells on the back side of the test modules (Table 2).

3.6. Flasher tests

A so-called flasher test is the extended analysis of solar cells including I–V measurement. A single cell mini module is placed in the FCT-350 flash tester. This device generates the light irradiation intensity of the sun on earth's surface by using of a flash lamp, which corresponds approximately to 1000 W/m². For our test, the I_{sc} (short circuit current) value is important to correlate the flasher tests to the outdoor measurements. To evaluate the measurement, the minimodule (single cell) was first measured without a structured film at five different radiation entry angles (0°, 10°, 20°, 30° and 40°). Then the film was fixed on the back side of the module by glue and the measurements were repeated. The influence of the structure could be determined by comparing the measurements. The advantage of using the flasher device was, to reduce the required amount of film and adhesive.

3.7. Outdoor measurements

Outdoor measurements were carried out to match the simulation results and labor-tests with those of the real world and characterize the structured film under field conditions. For this test, a series product of a 40-cell module was used. The module measurements were performed with a characteristic curve meter, which outputs a power according to standard test conditions (STC). The conditions are 1000 W/m² irradiation and 25°C module temperature. For referencing, the module is first aligned to the sun without film and the short-circuit current and solar irradiance are measured on the front and back sides. Then a 2 cm strip of the different films variants is glued on the back, at the intermediate areas between the cells, with adhesive 1 and aligned and measured perpendicular to the sun.

3.8. Economic efficiency analysis

To evaluate the cost-effectiveness of investing in the light-directing structure for PV application, the following criteria were identified as significant:

- Customer interest:

Current bifacial modules have an output of 310Wp. To generate customer interest, at least a jump to the next higher power class should be achieved. A power jump can be calculated with +10 Watt. This would mean a 3.3% increase in power.

- Wp price:

This should not increase significantly - at best not at all - due to the additional work steps and the additional components.

4. Results

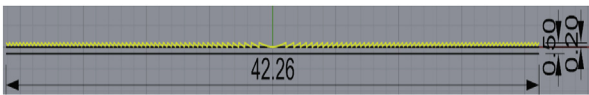
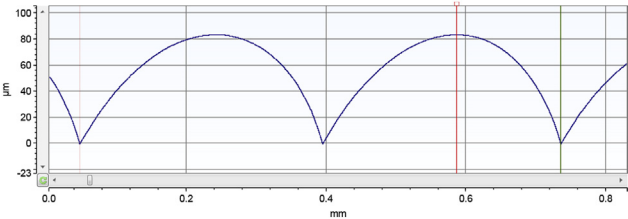
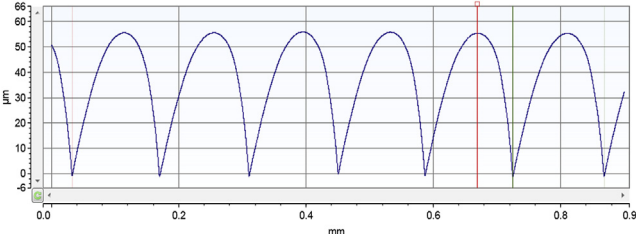
4.1. Simulations

Fig. 4 shows an exemplary simulation run. In contrary to the 3D layout, the 2D layout was performed always with mounted film on two sides. Since the software always references the sun's rays perpendicularly to the drawings' zero point (0,0,0), the geometry had to be rotated to run the simulation at different angles of incidence.

To determine the influence of a light-guiding film, a reference calculation series was done without it. For this series, the Irradiation angle from midday to evening (tilt_y) and the declination of the sun from summer to winter were varied (tilt_x). As basis of the results, it can be seen that the amount of absorbed light rays on the solar cell follows the ray incidence angle of the passing sun (Fig. 5).

As shown in Fig. 6, most of the sunlight is absorbed in the first 50 μm. A change in the angle of incidence from 30° has the effect

Table 2
Test structure list.

Film name	Structure
White backsheet ECOCAN LED-Booster	No structure 
Lenstar 75LPI	
Makrofol LM297	

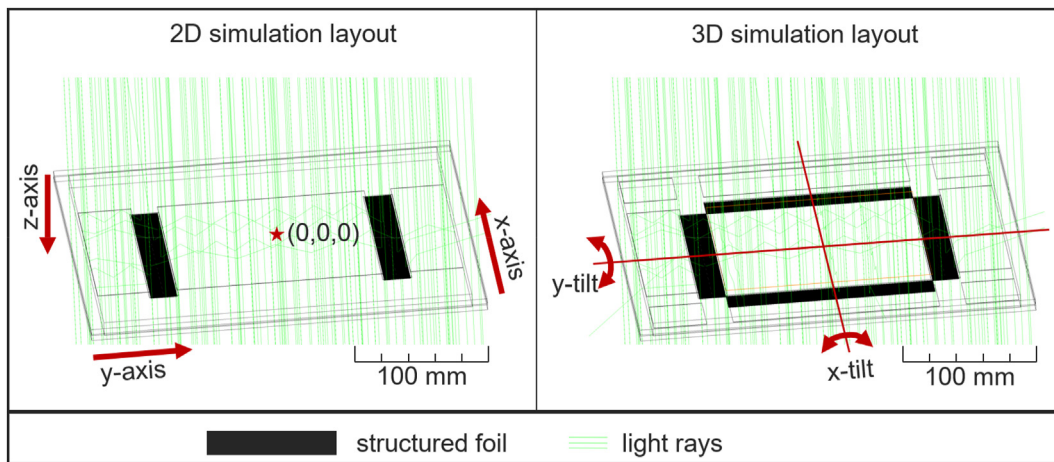


Fig. 4. 2D and 3D simulation layout.

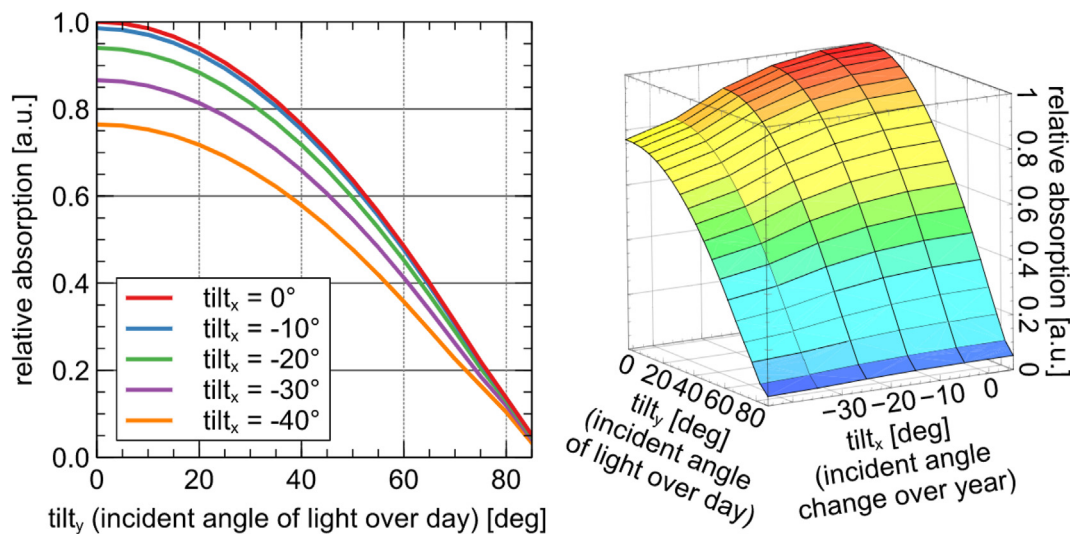


Fig. 5. Reference measurements for variation of irradiation angle.

that 12% less absorption occurs in this area.

Adding a 10 mm wide film with a prism structure to the geometry, the light absorption at the edges of the bottom side increases. This is a result of the light-guidance effect, where light rays that do not hit the active cell area and are redirected to it. If the sum of the absorption is calculated along the thickness of the cell and the result is applied across the width of the cell, the effect becomes clearly visible. This results in an elevated power absorption of about 1.5 mW/mm³ (Fig. 7).

The change of the incidence angle increases the light guidance effect, especially on the module side averted from direct light radiation. At a tilt angle above 30°, the additional gain of power with applied film is only in the range of 0.3% compared to a cell without film. The impact on the additionally absorbed power when using a light guidance film is shown in Fig. 8. Comparing the measurements of three commercial structured films to the reference simulation (without prism structure), the impact of the mini-prismatic structure can be recognized, especially at small angles of incidence (0° until 20°). Furthermore, it is obvious that already by scattering the light with commercial films, a profit in power resorption can be achieved, but not to the same magnitude as it was possible with the prism structure.

After evaluating the effect of varied angles of incidence with a constant film width, it became also important to evaluate the influence of variations the film width that was placed over the cell area. To get a theoretical estimate, the width of the film was varied and simulated from 2 mm to 32 mm. Based on a graphic representation of the light control, there are, under ideal conditions, three possibilities how the rays can be deflected and reach the active area of the solar cell for the first time (Fig. 7):

- structureE to back side of cell
- structureE -> total reflection -> Front Side of cell
- Structure -> total reflection -> total reflection -> Front Side of cell

In the consideration of the ongoing path of the light rays, those are either totally reflected back into the cell with reduced energy or completely deflected to the outside.

The results of the simulation have shown that the rays reaching the structure within 15 mm from the solar cell edge have all three deflection variants. From then on and up to 27 mm there is no direct deflection to the underside of the solar cell. If the rays move further away from the solar cell, they only reach the cell via at least two

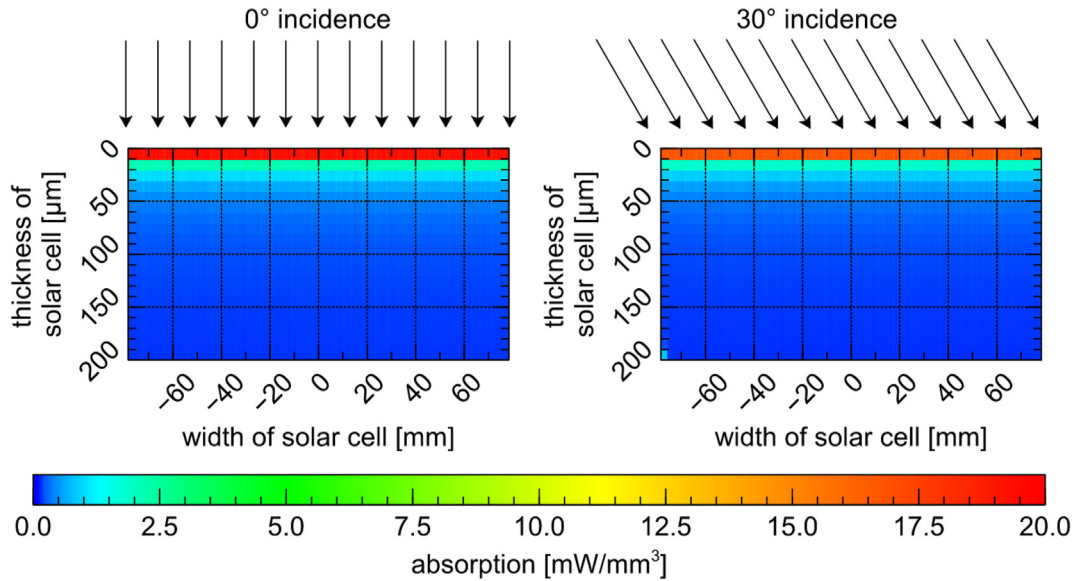


Fig. 6. Absorption on solar cell without film.

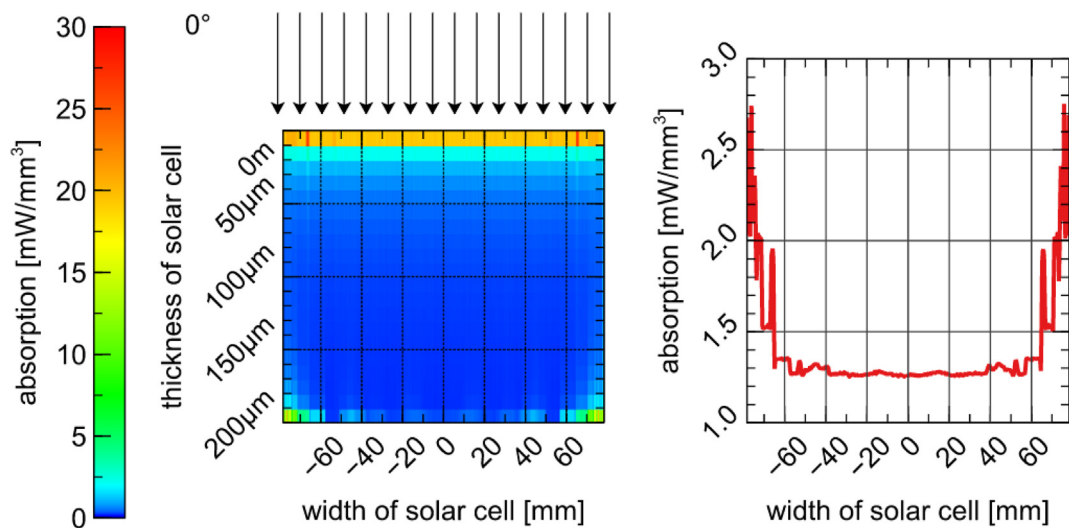


Fig. 7. Absorption on solar cell with film at 0°.

total reflections. This results in a decrease of absorbed power and leads to a plateau (Fig. 9).

Based on the simulation results described above, the following simulation results could be analyzed. The angle of incidence of the light was varied between 0° and ±20° and the beam path was displayed. By comparing the following pictures (Fig. 10 & Fig. 11), the rays that directly hit the solar cell (red rays) hardly change. If, however, the rays hit the structured film and are deflected, a change in the angle of incidence of the light already leads to no more directional beam guidance and reduces possible absorption when the rays are deflected directly to the back side (green rays). This also applies to beams that are totally reflected either 1 time (blue) or twice.

Although the structure designed for the perpendicular angle of incidence causes a redirection despite the changed angle of incidence, the number of rays that are redirected onto the solar cell decreases and thus also the absorption.

4.2. Material analysis – check of suitability

Fig. 12 shows the hemispheric and diffuse transmittance spectra of the investigated materials. All materials exhibit high transparency in the wavelength region between 300 and 1100 nm, showing values higher than 90%, and therefore meet the requirements. Significant absorptions were only found for PA12, PMMA and PC in the wavelength region below 400 nm due to their UV stabilization. Table 3 summarizes the measured haze values for the polymer films. Except for PP; all materials have haze values well below the specified 5%, indicated low light scattering. PP however showed a haze value of 84%, indicating that the major part of the transmitted light is scattered, making an effective light guidance nearly impossible. A possible explanation would be light scattering mainly caused by the crystalline zones within the polymer combined with surface roughness effects [21,22]. As a consequence, PP was excluded from further studies.

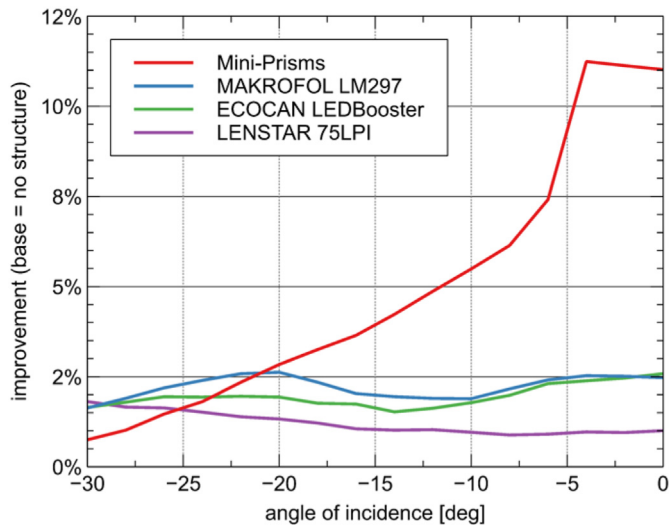


Fig. 8. Absorption-difference using structured films.

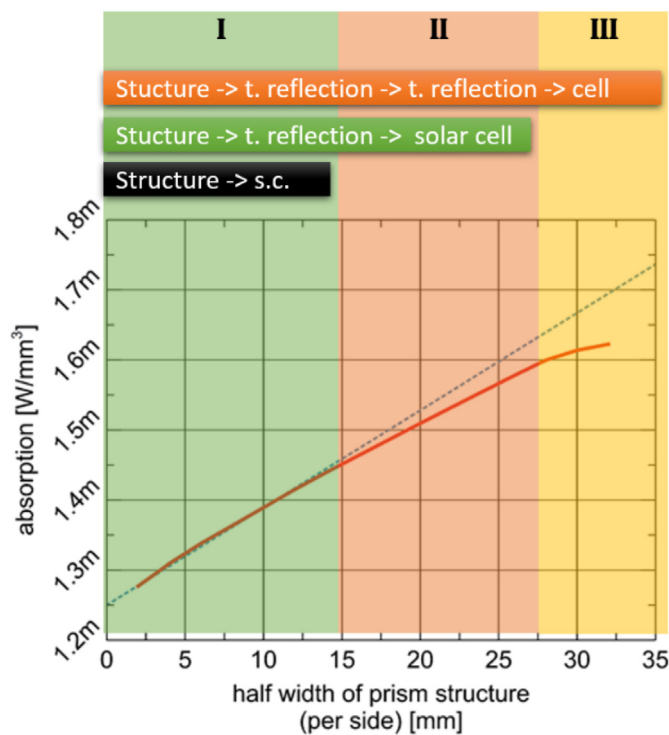


Fig. 9. Light path over cell width.

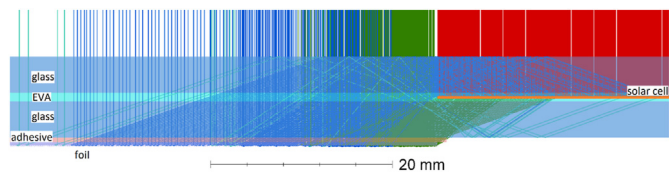


Fig. 10. Redirection at a perpendicular angle of incidence.

Fig. 13 shows the direction-dependent thermal expansion of PA12, PC and PMMA. PA12 shows a more or less constant and isotropic thermal expansion up to the glass transition temperature

at 50 °C, with CTE values around 100 ppm. Above glass transition a highly anisotropic expansion behavior was observed, leading to strong shrinkage in machine direction (MD) and strong expansion in transversal direction (TD). A similar behavior was found for PMMA, with isotropic behavior up to 70 °C, followed by shrinkage in the extrusion direction (MD) and slight expansion in the transverse direction (TD) at higher temperatures. The glass transition temperatures of the investigated PMMA and PA12 films is within the operating temperature range of PV modules, hence the observed anisotropic thermal expansion behavior is considered problematic for the intended use as light guidance film. Firstly, the anisotropic thermal expansion probably reduces the light guidance efficiency. And secondly, because of the adhesive bond to the PV module glazing, excessive thermal expansion assumedly causes internal stresses, which over time would eventually lead to delamination. Additionally, certification according to IEC 61215 will be most probably challenging, as the whole module including the applied structured film has to withstand 1000 h of damp heat test conditions (85 °C and 85% relative humidity). In comparison, PC exhibits nearly isotropic behavior, showing a more or less constant thermal expansion with CTE values between 60 and 70 ppm up to a temperature of 130 °C. Only then shrinkage sets in due to reaching the glass transition temperature. Based on these results, PC was selected as the most promising candidate material for light guidance films, and subsequently used for assessment of the different adhesives.

The polyurethane-based two-component adhesive (Adhesive 2) was easy to apply, due to medium viscosity of the material provided in handy cartridges, no bubble accuracy. However, after the specified curing time, only very low adhesion between glass and PC was detectable (>0.5 N/mm). The two-component silicone system (Adhesive 4; one high and one low viscosity component) formed bubbles during mixing and without vacuum they vanished very slowly. Application proved to be difficult, and due to the viscosity and tackiness no homogeneous coating could be obtained. It was not possible to produce useable samples for the peel test. In contrast, the second two-component silicone system (Adhesive 5), with lower viscosity, also showed bubbles after mixing but with quick disappearance. Nevertheless, the results of the peel test of Adhesive 5 showed very weak adhesion (approx. 0.5 N/mm) between glass and PC. First UV aging test results indicate a trend that exposure to light slightly improves adhesion. The third tested silicone system, Adhesive 1, appears in a very high viscosity and therefore it is challenging to apply it in a thin layer. But the adhesive properties are very good (10 mm/N). Also, after short irradiation an increase in adhesion was observed. An explanation for the increase of the adhesion after exposure to light could be the completion of the crosslinking processes due to triggering of incorporated catalysts [23]. Adhesive 3 gives appropriate peel test results in the range of 11 N/mm and is easy in handling and applying of the adhesion layer. Concerning the optical properties of the two good performing Adhesives (1 and 3), Adhesive 3 shows better transparency (with 86%) than Adhesive 1 (with 81%) measured on glass (with 90%). Based on the obtained results, Adhesive 3 was chosen for further testing.

4.3. Effect of light guidance film

To evaluate the light directing effect of the developed film, tests were first performed with the commercial film Makrofol LM297 and the white back sheet. The commercial film was chosen because it had the best results in the simulation. For the test, the LM297 film was cut into 1, 1.5 and 2 cm wide strips. These were glued to the edges of a single cell test module on its back side and measured with the flasher tester. By changing the angle of the sample to the light source, this influence could also be measured. As a reference

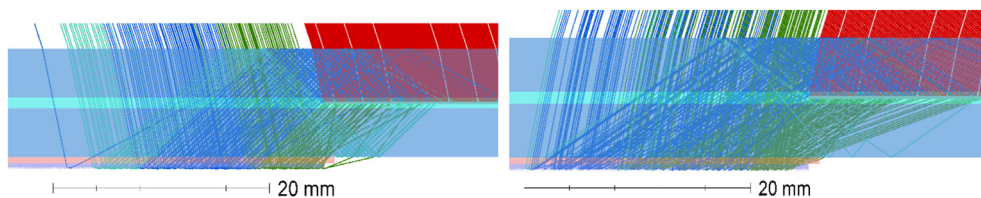


Fig. 11. Redirection at -20° (left) and $+20^\circ$ (right) angle of incidence.

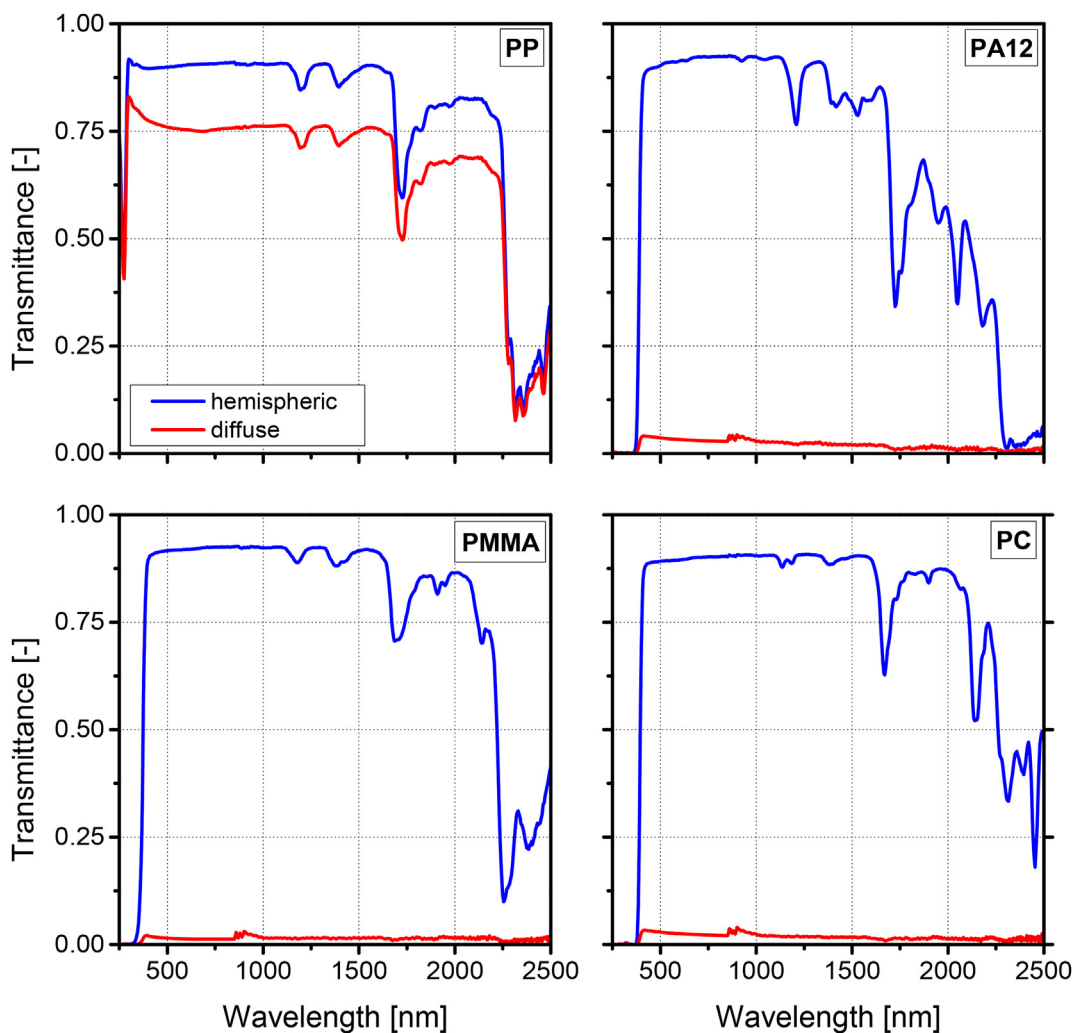


Fig. 12. Hemispheric and diffuse transmittance spectra of the investigated materials.

Table 3
Hemispheric transmittance and haze values of investigated polymer films.

Film	Thickness	Haze
PP	510 μm	84.1 \pm 0.1%
PA12	600 μm	3.5 \pm 0.9%
PMMA	510 μm	1.6 \pm 0.2%
PC	500 μm	3.0 \pm 1.2%

measurement, the sample was measured without the film applied. Fig. 14 shows that, as already documented from the simulation results, a wider structure increases the absorption. Furthermore, it is visible that at angles of incidence $>20^\circ$, at 2 cm width of the film, the gain increases and does not decrease as simulated. This

behavior can be explained by the effect of scattering from this angle of incidence. An overlap of the film over the solar cell has an additional positive effect on the absorption amount. Most importantly, the use of a white back sheet, of the same width, achieves a higher gain than the commercial film. The reason for this is the diffuse reflection of the white surface, which does not have a directional preference like a structured film. Due to the test results and the shortage of material, the width of the films was fixed at 2 cm for the next tests.

After the production, several variants of the film with the light-directing structure, 2 cm wide strips of three variants were glued to the test module and measured with the flash tester. For better comparison, the results of the commercial film and the back sheet were added to the graph below (Fig. 15).

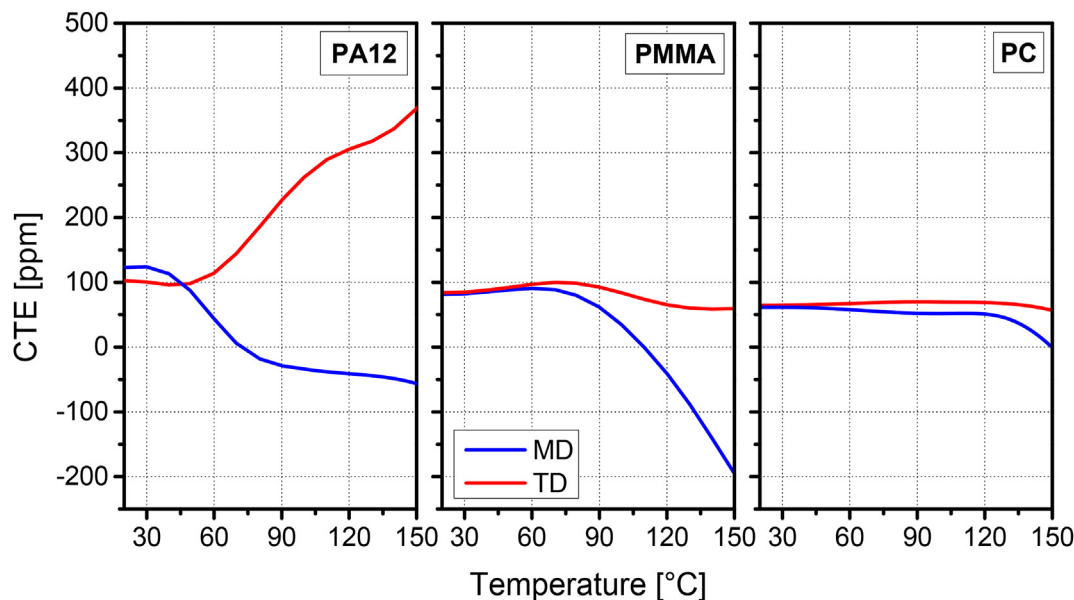


Fig. 13. Thermal expansion behavior of PA12, PMMA and PC, measured in machine direction (MD, blue lines) and transversal direction (TD, red lines).

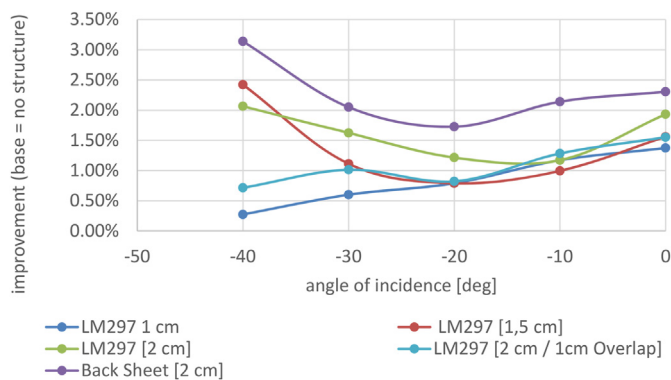


Fig. 14. Reference measurements (Makrofol LM297 and white Back sheet).

The extruded film V3 was noticeably worse than the commercial film. By optimizing the roll geometry and adjusting the process parameters (temperature, pressure), the light-directing effect could be improved. Compared to the reference measurements, the gain due to light guiding is clearly visible up to an angle of incidence of >20°. As the angle increases, variant 5.1 behaves as described by the simulation, but variant 6.2 even increases slightly.

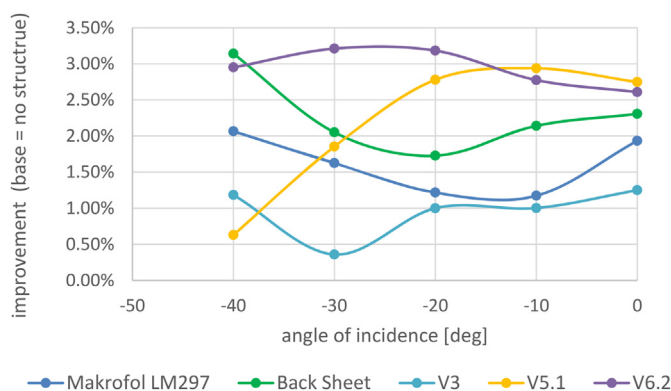


Fig. 15. Flasher Test structured film.

To verify the laboratory measurements, the three versions of the structured film were now bonded to the back of a standard 40-cell module with large cell spacing and measured outdoors. Since bifacial modules convert light from the front as well as from the back side into power, an additional correction factor had to be considered (P_{mpp} corrected). Using this factor, measurements taken on different days can now be compared. Table 4 shows the results of the measurements performed. The mean value of three measurements was always used for this purpose. All films selected for this test exhibited a measured additional gain due to the light-directing film within the error tolerance. However, the simulation results could not be achieved.

The deviations of the indoor and outdoor measurements from the simulation results can be attributed to the roughness not considered in the simulation and the not accurately reproduced geometry. If the roughness values in Table 5 of the two structures are compared, it is obvious that the larger value for V6.2 favors scattering at the larger angles of incidence and thus leads to higher absorption. Furthermore, however, too high a roughness, see film V3, is counterproductive. Only two of the structures and the silicone cast had a surface roughness around 10 μm .

The different roughness values are due to the material to be extruded, the surface of the roll and the variation of the parameters during extrusion (see Table 6). The use of a matted roll surface is preferable, as this lowers the roughness. Furthermore, an increased pressure between the stamping roll and the textured roll should be avoided. The influence of the temperature of the forming roll could not be clearly identified based on the available data.

The second reason for the non-achievement of the simulation results was the deviation from the desired geometry. To examine this, the geometry of the manufactured films was measured using a profilometer. The results show that only the silicone cast has an almost perfect reproduction of the desired structure. All others achieve at best and on average only half the geometric height. There are also differences in the pattern over the entire film width (Fig. 16). To improve the stamping process, it would be necessary to switch from the lab system to a production system. This would allow a larger temperature and pressure range to be used for the best possible forming of the geometry. For this change, a larger structure roll would have to be manufactured.

Table 4
Outdoor measurement results.

Measurement ID	$P_{mpp}[W_p]$	Irradiance Quotient Back to Front	Correction factor to ref.	P_{mpp} corrected $[W_p]$	Gain [%]
Reference	207.8	0.1	0	207.8	0
Film V3	207.8	0.09	1.020	212.16	2.1
Film V5.1	200.7	0.077	1.033	213.57	2.9
Film V6.2	205.2	0.071	1.039	213.52	2.7

Table 5
Structure roughness.

Type	$Ra[\mu m]$ slope	$Ra[\mu m]$ top
Silicon	9.9	–
V3	22.4	1.6
V4	17.5	1.6
V5.1	10.2	1.6
V5.2	18.3	10.2
V5.3	16.7	1.7
V5.4	16.3	1.7
V6.1	12.8	2.2
V6.2	13.4	2.3
V6.3	10.1	1.5
V6.4	14.5	1.1

Table 6
Extruder process parameters.

Version	Roll surface	Temperature $[^{\circ}C]$	Pressure [bar]	Speed [R/min]
V5.1	smooth	Standard	4	1,2
V5.2	smooth	+10	4	1,2
V5.3	smooth	Standard	8	1,2
V5.4	smooth	-20	8	1,2
V6.1	matt	Standard	4	1,2
V6.2	matt	Standard	4–6	0,7
V6.3	matt	+20	4	0,7
V6.4	matt	+20	4	0,7

Based on the tests carried out, it is evident that the developed structure can be used to direct the light and thus increase the module efficiency. Optimization of the structure over the entire width of the film would visibly increase the gain. An important result is also the influence of the roughness on the light guidance. This parameter could be adjusted in such a way that an optimal benefit can be generated depending on the installation site. Thus,

Table 7
Listing of the costs due the additional efforts.

Category	Description	Price[€]/Module
Workload	2 person for 20 min	16
Glue	13,26 €/350 ml (6,6 g/Module)	0.25
Film	PC = 20 €/kg	0.13
Sum	Additional costs per module	16.38

for example Greenhouses by a low roughness the light is redirected especially over the midday to prevent too large heat inputs and to let the light through in the remaining time. For the application as a carport, a higher roughness would reduce the maximum gain, but increase the average over the day.

4.4. Economic efficiently analysis

For the analysis, Ottoseal S50 was assumed to be the adhesive, since it was evaluated as having the best performance in terms of processing and durability. The work involved is the application of the adhesive and the positioning of the foil.

The Table 7 shows that personnel costs have a major financial impact. If the production costs (100 € = fictitious value) and the sales price is compared, the profitability of a product is obtained. The following Table 8 compares a standard module and modules with structured film with 3% or 11% additional profit.

As mentioned before, the cost of Workload has a great influence. To maintain the economic viability of a PV module enhanced by light guidance film, the additional cost should not exceed 12.7 € at 3% and 4,6 € at 11%. This would certainly be possible by improved or automated processing of the film possible.

In terms of the power classes mentioned, the 3% would not be enough for the next level and at 11% the module would be specified at 340Wp and would therefore give away 1.3%. Based on the results,

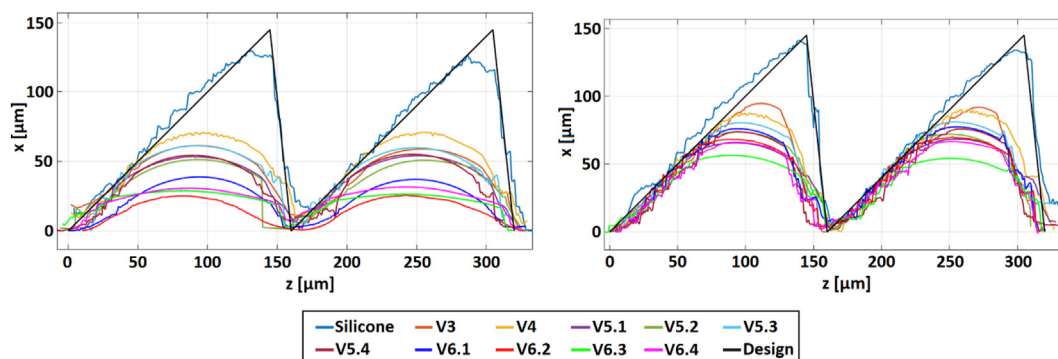


Fig. 16. Geometrical Structural stability (left: middle position, right: border).

Table 8
Profitability.

Module type	Production costs [€]	Sales price [€]	Profitability
310Wp standard	100	170	1,7
310Wp + 3% (319Wp)	100 + 16	175,61	1,5
310Wp + 11% (344Wp)	100 + 16	189,25	1,6

the economic efficiency is questionable with an additional gain of only 3%.

5. Conclusions

Based on simulations, it was shown that the use of a structured film with a width of up to 30 mm results in increased absorption in the edge areas. Furthermore, the angle of incidence of the sun's rays is a non-negligible factor due to the fixed structural geometry. In comparison to commercial structures and dependent angles of incidence, however, an additional gain of up to 11% could be simulated.

Based on material tests performed to verify compliance with the specifications for use in photovoltaics, PC was evaluated as the preferred film material. Only this material could comply sufficiently with both factors, i.e. transparency and dimensional stability. Furthermore, a single-component silicone adhesive, which is necessary for the connection between the film and the PV module, was convincing in the stripping test. Despite its high viscosity, a more homogeneous surface was achieved compared to the other adhesives.

During the evaluation of the produced films (extruding) it became clear that there were difficulties in the exact shaping of the structure. Although various parameters of the process were adjusted, it was not possible to achieve 100% structural fidelity. Optimization would also be necessary regarding roughness and structure stability, as these have the major influences on light guidance. Due to the difficulties mentioned above, the desired results of the simulation could not be achieved in the laboratory or outdoor tests. Nevertheless, the positive influence of the light-guidance structure could be confirmed. However, a gain of at least 3.3% would be necessary for the film to be commercially viable.

CRedit authorship contribution statement

Markus Zauner: Conceptualization, Methodology, Investigation, Resources, Writing – original draft. **Wolfgang Muehleisen:** Validation, Formal analysis, Investigation, Writing – review & editing. **Dominik Holzmann:** Validation, Investigation. **Marcus Baumgart:** Validation, Formal analysis, Writing – review & editing. **Gernot Oreski:** Conceptualization, Methodology, Formal analysis, Writing – original draft, Writing – review & editing. **Sonja Feldbacher:** Validation, Formal analysis, Investigation, Resources, Writing – original draft. **Markus Feichtner:** Validation, Resources. **Wolfgang Nemitz:** Validation, Formal analysis. **Claude Leiner:** Validation. **Christian Sommer:** Conceptualization, Formal analysis, Writing – original draft, Writing – review & editing, Project administration. **Frank Reil:** Validation, Formal analysis, Investigation.

Declaration of competing interest

The authors declare that they have no known competing financial interests or personal relationships that could have appeared to influence the work reported in this paper.

Acknowledgement

The authors gratefully acknowledge financial support from the BMVIT within the “Production der Zukunft” program of the Austrian Research Promotion Agency (FFG), which has been done in the project “Next_pro_Foil” (864852).

References

- [1] Schmid C, Fuller E, MacBride B, Mickiewicz R, Kinsey GS, Zhou J, Chakravarti S, Kodis A. AnGLE of incidence performance study of PV modules with patterned polycarbonate front sheets. In: Proceedings of 28th European Photovoltaic Solar Energy Conference and Exhibition, pp. 3090–3092.
- [2] Backes A, Adamovic N, Schmid U. New light management concepts for standard Si solar cells fabricated by embossing of polycarbonate front & back sheets. In: 28th European Photovoltaic Solar Energy Conference and Exhibition, pp. 3096–3098.
- [3] K. Drabczyk, P. Sobik, Z. Starowicz, K. Gawlińska, A. Pluta, B. Drabczyk, Study of lamination quality of solar modules with PMMA front layer, *MI* 36 (3) (2019) 100–103, <https://doi.org/10.1108/MI-12-2018-0087>.
- [4] L. Kuna, G.C. Eder, C. Leiner, G. Peharz, Reducing shadowing losses with femtosecond-laser-written deflective optical elements in the bulk of EVA encapsulation, *Prog. Photovoltaics Res. Appl.* 23 (9) (2015) 1120–1130, <https://doi.org/10.1002/ppp.2530>.
- [5] B. Lamprecht, V. Satzinger, V. Schmidt, G. Peharz, F.P. Wenzl, Spatial light modulator based laser microfabrication of volume optics inside solar modules, *Opt Express* 26 (6) (2018) A227–A239, <https://doi.org/10.1364/OE.26.00A227>.
- [6] H. Holst, H. Schulte-Huxel, M. Winter, S. Blankemeyer, R. Witteck, M.R. Vogt, T. Booz, F. Distelrath, M. Köntges, K. Bothe, R. Brendel, Increased light harvesting by structured cell interconnection ribbons: an optical ray tracing study using a realistic daylight model, *Energy Procedia* 92 (2016) 505–514, <https://doi.org/10.1016/j.egypro.2016.07.134>.
- [7] W. Muehleisen, L. Neumaier, C. Hirschl, T. Maier, M. Schwark, S. Seufzer, R. Battistutti, M. Pedevilla, J. Scheurer, R. Lorenz, Comparison of output power for solar cells with standard and structured ribbons, *EPJ Photovolt* 7 (2016) 70701, <https://doi.org/10.1051/epjpv/2016003>.
- [8] G. Oreski, G.C. Eder, Y. Voronko, A. Omazic, L. Neumaier, W. Muehleisen, G. Ujvari, R. Ebner, M. Edler, Performance of PV modules using co-extruded backsheets based on polypropylene, *Sol. Energy Mater. Sol. Cell.* 223 (2021) 110976, <https://doi.org/10.1016/j.solmat.2021.110976>.
- [9] V.D.M.A. International, *Technology Roadmap for Photovoltaic (ITRPV): 2019 Results*, 2020.
- [10] Sng E, Ang CX, Lim I. Investigation and analysis of bifacial photovoltaics modules with reflective layer. In: 35th European Photovoltaic Solar Energy Conference and Exhibition, pp. 1260–1264.
- [11] M.R. Vogt, H. Holst, H. Schulte-Huxel, S. Blankemeyer, R. Witteck, P. Bujard, J.-B. Kues, C. Schinke, K. Bothe, M. Köntges, R. Brendel, PV module current gains due to structured backsheets, *Energy Procedia* 124 (2017) 495–503, <https://doi.org/10.1016/j.egypro.2017.09.286>.
- [12] C. Leiner, F.P. Wenzl, C. Sommer, G. Peharz, Improving the effectiveness of photovoltaic devices by light guiding optical foils, in: R. Winston, J.M. Gordon (Eds.), *Nonimaging Optics: Efficient Design for Illumination and Solar Concentration XIII—Commemorating the 50th Anniversary of Nonimaging Optics*, SPIE, 2016, p. 995508.
- [13] P. Kärhä, H. Baumgartner, J. Askola, K. Kylmänen, B. Oksanen, K. Maham, V. Huynh, E. Ikonen, Measurement setup for differential spectral responsivity of solar cells, *Opt. Rev.* 27 (2) (2020) 195–204, <https://doi.org/10.1007/s10043-020-00584-x>.
- [14] M. Koehl, M. Heck, S. Wiesmeier, J. Wirth, Modeling of the nominal operating cell temperature based on outdoor weathering, *Sol. Energy Mater. Sol. Cell.* 95 (7) (2011) 1638–1646, <https://doi.org/10.1016/j.solmat.2011.01.020>.
- [15] C.-H. Chien, T. Chen, F.-I. Su, C.-Y. Lin, T.-H. Su, Y.-M. Lin, Y.-C. Liu, T.-L. Tsay, Thickness effects on the thermal expansion coefficient of indium tin oxide/polyethylene terephthalate film, *Exp. Tech.* 40 (2) (2016) 639–644, <https://doi.org/10.1007/s40799-016-0065-1>.
- [16] D.H. Jeon, K.H. Lee, H.J. Park, The effects of irradiation on physicochemical characteristics of PET packaging film, *Radiat. Phys. Chem.* 71 (5) (2004) 1059–1064, <https://doi.org/10.1016/j.radphyschem.2003.10.009>.
- [17] B. Hirschmann, G. Oreski, G. Pinter, Thermo-mechanical characterisation of fluoropolymer films for concentrated solar thermal applications, *Sol. Energy Mater. Sol. Cell.* 130 (2014) 615–622, <https://doi.org/10.1016/j.solmat.2014.08.013>.
- [18] F. Hild, S. Roux, Digital image correlation: from displacement measurement to identification of elastic properties - a review, *Strain* 42 (2) (2006) 69–80, <https://doi.org/10.1111/j.1475-1305.2006.00258.x>.
- [19] A.M. Korsunsky, M. Sebastiani, E. Bemporad, Residual stress evaluation at the micrometer scale: analysis of thin coatings by FIB milling and digital image correlation, *Surf. Coating. Technol.* 205 (7) (2010) 2393–2403, <https://doi.org/10.1016/j.surfcoat.2010.09.033>.
- [20] E. Appendix, AM1.5 reference solar spectrum, in: C.J. Chen (Ed.), *Physics of Solar Energy*, John Wiley & Sons, Inc, Hoboken, NJ, USA, 2011, pp. 307–312.
- [21] K. Resch, G.M. Wallner, C. Teichert, G. Maier, M. Gahleitner, Optical properties

- of highly transparent polypropylene cast films: influence of material structure, additives, and processing conditions, *Polym. Eng. Sci.* 46 (4) (2006) 520–531, <https://doi.org/10.1002/pen.20503>.
- [22] K. Resch, G.M. Wallner, C. Teichert, M. Gahleitner, Highly transparent polypropylene cast films: relationships between optical properties, additives, and surface structure, *Polym. Eng. Sci.* 47 (7) (2007) 1021–1032, <https://doi.org/10.1002/pen.20781>.
- [23] M. Gallo, R.G. Rinaldi, The effect of pre-curing UV -irradiation on the cross-linking of silicone rubber, *J. Appl. Polym. Sci.* 138 (6) (2021) 49807, <https://doi.org/10.1002/app.49807>.